Biphasic regulation of $InsP_3$ receptor gating by dual Ca^{2+} release channel BH3-like domains mediates Bcl-x_L control of cell viability

Jun Yang[a,b,1], Horia Vais[b], Wenen Gu[a], and J. Kevin Foskett[b,c,1]

[a]Key Laboratory of Reproduction Regulation of the National Population and Family Planning Commission, Shanghai Institute of Planned Parenthood Research, Shanghai 200032, China; [b]Department of Physiology, Perelman School of Medicine, University of Pennsylvania, Philadelphia, PA 19014; and [c]Department of Cell and Developmental Biology, Perelman School of Medicine, University of Pennsylvania, Philadelphia, PA 19014

Edited by Andrew R. Marks, Columbia University College of Physicians & Surgeons, New York, NY, and approved February 18, 2016 (received for review September 10, 2015)

Antiapoptotic Bcl-2 family members interact with inositol trisphosphate receptor ($InsP_3R$) Ca^{2+} release channels in the endoplasmic reticulum to modulate Ca^{2+} signals that affect cell viability. However, the molecular details and consequences of their interactions are unclear. Here, we found that Bcl-x_L activates single $InsP_3R$ channels with a biphasic concentration dependence. The Bcl-x_L Bcl-2 homology 3 (BH3) domain-binding pocket mediates both high-affinity channel activation and low-affinity inhibition. Bcl-x_L activates channel gating by binding to two BH3 domain-like helices in the channel carboxyl terminus, whereas inhibition requires binding to one of them and to a previously identified Bcl-2 interaction site in the channel-coupling domain. Disruption of these interactions diminishes cell viability and sensitizes cells to apoptotic stimuli. Our results identify BH3-like domains in an ion channel and they provide a unifying model of the effects of antiapoptotic Bcl-2 proteins on the $InsP_3R$ that play critical roles in Ca^{2+} signaling and cell viability.

Bcl-2 | ion channel | calcium | apoptosis | mitochondria

The inositol trisphosphate receptors ($InsP_3R$) are a family of intracellular cation channels that release Ca^{2+} from the endoplasmic reticulum (ER) in response to a variety of extracellular stimuli (1). Three $InsP_3R$ isoforms are ubiquitously expressed and regulate diverse cell processes, including cell viability (1). Activation of the channels by $InsP_3$ elicits changes in cytoplasmic Ca^{2+} concentration ($[Ca^{2+}]_i$) that provide versatile signals to regulate molecular processes with high spatial and temporal fidelity (1). Regions of close proximity to mitochondria enable localized Ca^{2+} release events to be transduced to mitochondria (2, 3). Ca^{2+} released from the ER during cell stimulation modulates activities of effector molecules and is taken up by mitochondria to stimulate oxidative phosphorylation and enhance ATP production (4–6) to match energetic supply with enhanced demand. In addition, cells in vivo are constantly exposed to low levels of circulating hormones, transmitters, and growth factors that bind to plasma membrane receptors to provide a background level of cytoplasmic $InsP_3$ (7) that generates low-level stochastic $InsP_3R$-mediated localized or propagating $[Ca^{2+}]_i$ signals (8–10). Such signals also play an important role in maintenance of cellular bioenergetics (8). Nevertheless, under conditions of cell stress the close proximity of mitochondria to Ca^{2+} release sites may result in mitochondrial Ca^{2+} overload and initiate Ca^{2+}-dependent forms of cell death, including necrosis and apoptosis (11–13). It has been suggested that high levels of ER Ca^{2+} (14–16) and enhanced activity of the $InsP_3R$ (17–19) promote cell death by providing a higher quantity of released Ca^{2+} to mitochondria (3, 20, 21).

Protein interactions modulate the magnitude and quality of $InsP_3R$-mediated $[Ca^{2+}]_i$ signals that regulate apoptosis and cell viability. Notable in this regard is the Bcl-2 protein family. Proapoptotic Bcl-2–related proteins Bax and Bak initiate cytochrome C release from mitochondria in response to diverse apoptotic stimuli, whereas antiapoptotic Bcl-2–related proteins, including Bcl-2 and Bcl-x_L, antagonize Bax/Bak by forming heterodimers that prevent their oligomerization and apoptosis initiation (22, 23). Heterodimerization is mediated by interactions of proapoptotic Bcl-2 homology 3 (BH3) domains with a hydrophobic groove on the surface of antiapoptotic Bcl-2 proteins (23) that is a therapeutic target in diseases, including cancer (22). Whereas a central feature of molecular models of apoptosis is the control of outer mitochondrial membrane permeability by Bcl-2–related proteins, a substantial body of evidence has demonstrated that these proteins localize to the ER (24, 25), bind to $InsP_3Rs$ (26–32) and, by modulating $InsP_3R$-mediated Ca^{2+} release, regulate ER-mediated cell death and survival (15, 27, 32–34). Nevertheless, a unified understanding of the detailed molecular mechanisms by which Bcl-2 family proteins interact with and regulate $InsP_3R$ channel activity is lacking. The Bcl-2 family member homolog NrZ interacts with the amino-terminal $InsP_3$-binding region via its helix 1 BH4 domain and inhibits Ca^{2+} release (28). Bcl-2 also interacts with the $InsP_3R$ (26) via its BH4 domain (35), but in contrast it associates with a region in the central coupling domain (35). Whereas this interaction also inhibits Ca^{2+} release (26), Bok interacts with the channel 500 residues C-terminal to the Bcl-2 binding sequence via its BH4 domain but does not affect Ca^{2+} release (29). Conversely, the Bcl-x_L BH4 domain may lack this interaction (36). Inhibition of the Bcl-2 BH4 domain interaction with the channel enhanced $InsP_3R$-mediated Ca^{2+} signals and apoptosis sensitivity in white blood cells (18, 35, 37).

Significance

Changes in Ca^{2+} concentration in the cell play important roles in cell life and death decisions. Antiapoptotic Bcl-2 family proteins help protect cells from dying by interacting with proteins at mitochondria and endoplasmic reticulum. At the endoplasmic reticulum, antiapoptotic Bcl-2 proteins interact with $InsP_3R$ Ca^{2+} channels that release Ca^{2+} into the cytoplasm. However, it is controversial how they interact with the $InsP_3R$, as well as the functional consequences of the interactions. We found that antiapoptotic Bcl-x_L interacts with $InsP_3Rs$ by unique mechanisms that change the activity of the channel depending on its concentration. We also found that disrupting these interactions diminishes cell viability. Our results provide a unifying model of the effects of antiapoptotic Bcl-2 proteins on the $InsP_3R$.

Author contributions: J.Y., H.V., and J.K.F. designed research; J.Y., H.V., and W.G. performed research; J.Y. contributed new reagents/analytic tools; J.Y., H.V., and J.K.F. analyzed data; and J.Y. and J.K.F. wrote the paper.

The authors declare no conflict of interest.

This article is a PNAS Direct Submission.

[1]To whom correspondence may be addressed. Email: junyangsd@yahoo.com or foskett@mail.med.upenn.edu.

This article contains supporting information online at www.pnas.org/lookup/suppl/doi:10.1073/pnas.1517935113/-/DCSupplemental.

However, it is unclear if Bcl-2 inhibits Ca^{2+} signaling directly by binding to the channel or if it acts indirectly, as a hub in a protein complex that influences channel phosphorylation (38). Conversely, we demonstrated that Bcl-x_L, Bcl-2, and Mcl-1 bind to the carboxyl (C)-terminus of all three $InsP_3R$ isoforms, and showed that these interactions activated single $InsP_3R$ channels and promoted $InsP_3R$-mediated Ca^{2+} release and apoptosis resistance (27, 31, 32). Furthermore, Bcl-x_L mediates an interaction of oncogenic K-RAS with the $InsP_3R$ C terminus that regulates its biochemical and functional interaction and cell survival (39). However, the molecular details of the interactions of antiapoptotic protein with the $InsP_3R$ C terminus are unknown. Furthermore, the relationship between Bcl-2 family protein binding in the coupling domain and C terminus is unclear. Thus, the mechanisms whereby Bcl-2 and Bcl-x_L affect $InsP_3R$ activity and the effects of this modulation on cell viability remain to be determined.

Here, we used single-channel electrophysiology of native ER membranes to explore the detailed mechanisms of the effects of Bcl-x_L on the $InsP_3R$, and the role of this interaction on cell viability. Surprisingly, our results reveal that whereas Bcl-x_L activates the channel at low concentrations, it inhibits it at higher concentrations, resulting in a biphasic response of channel activation on [Bcl-x_L]. Remarkably, the Bcl-x_L BH3 domain-binding pocket is required for both effects. Low [Bcl-x_L] activates the channel by simultaneous binding to two BH3 domain-like helices in the channel C terminus, whereas channel inhibition at high [Bcl-x_L] requires binding to only one of them and to a site previously identified as the Bcl-2 binding site in the channel-coupling domain. Disruption of these interactions diminishes cell viability. Our results provide a unifying model of the effects of antiapoptotic Bcl-2 proteins on the $InsP_3R$ that play critical roles in Ca^{2+} signaling and cell viability.

Results

Bcl-x_L Binds to Dual BH3-Like Domains in the $InsP_3R$ Carboxyl Terminus. The $InsP_3R$ consists of a 600-residue N-terminal $InsP_3$ binding domain, a cytoplasmic region (coupling domain) that links it to the transmembrane pore region that contains six transmembrane (TM) helices, and a cytoplasmic C-terminal tail of ∼175 amino acids (Fig. 1*A*) (1). The strength of the interaction of Bcl-x_L with a region spanning from the TM5–TM6 linker to the C terminus (residues 2,512–2,750) is quantitatively equivalent to that of the full-length channel (27, 31). To define Bcl-x_L binding determinants within this region, GST-fusion proteins (Fig. 1*B*) were immobilized on glutathione beads, the quantities of beads were titrated, and the amounts of GST-$InsP_3R$ fragments used for pull-down experiments as well as the concentrations of Bcl-x_L were adjusted to equivalent levels. Bcl-x_L bound to a construct containing TM6 and the C terminus (TM6+C; residues 2,571–2,750) as efficiently as to the longer construct used in refs. 27 and 31. However, a shorter construct that encompassed the terminal 7 residues of TM6 and the remaining C terminus (C-term; residues 2,589–2,750) bound Bcl-x_L less efficiently (Fig. 1*B*). The TM6 helix is predicted to form the channel gate near residue G2586 (Fig. 1*A*) and to extend beyond the membrane into the cytoplasm. Distal to this helix, the remaining C terminus is predicted to contain three additional helices (H2–H4). We defined H1 as the helix containing TM6 and the 14 subsequent residues. Constructs with either H1 (ΔH1) or H4 (ΔH4) deleted bound Bcl-x_L (Fig. 1*B*), whereas one encompassing only helices 2 and 3 failed to bind Bcl-x_L (Fig. 1*B*), suggesting that both H1 and H4 bind Bcl-x_L. In agreement, purified H1 or H4 peptides each interacted with GST-Bcl-x_L (Fig. 1*C*). The interaction of full-length $InsP_3R$ with Bcl-x_L was inhibited by purified H1 or H4 proteins in the pull-down lysate (Fig. 1*C*), indicating that, whereas either H1 or H4 can bind to Bcl-x_L, both are required for strong binding to full-length $InsP_3R$. This result also suggests that the C terminus is the dominant Bcl-x_L binding region in the $InsP_3R$.

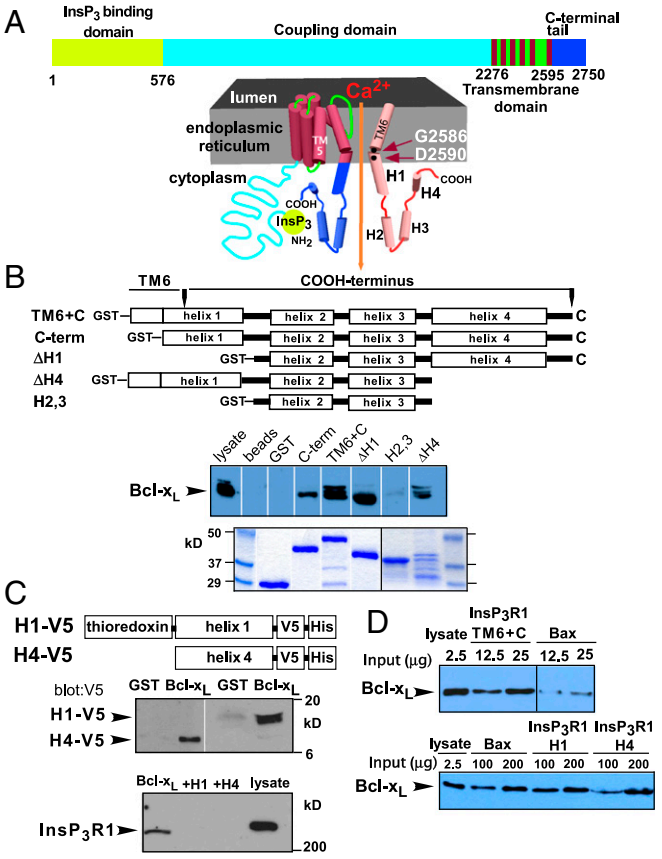

Fig. 1. Bcl-x_L binds differentially to two sites in the $InsP_3R$ C terminus. (*A*) Schematic of full-length $InsP_3R$ (*Upper*) and C terminus extending from approximately halfway down final transmembrane helix 6 (TM6) into cytoplasmic region containing four putative helices, H1–H4. From PSIPRED: TM6+C: residues 2,571–2,750; C-term: 2,591–2,750; H1: 2,571–2,606; H2: 2,627–2,644; H3: 2,658–2,678; H4: 2,690–2,732. (*B*) Schema of GST-fusion proteins used in Bcl-x_L pull-down assays. (*Upper*) Bcl-x_L pulled down; (*Lower*) Coomassie stain of GST fusion proteins. Multiple Bcl-x_L bands most likely represent amidated and deamidated forms (see ref. 51). (*C*) GST-Bcl-x_L pull down of V5-tagged purified H1 and H4 peptides (*Upper*). Binding of full-length $InsP_3R$ blocked by H1 and H4 peptides (*Lower*). (*D*) Bcl-x_L binds more strongly to $InsP_3R$ C terminus than to full-length human Bax (h-Bax) (*Upper*). Binding of Bcl-x_L to GST-Bax and GST-H1 is comparable, whereas binding to GST-H4 is weaker (*Lower*).

The affinity of the C terminus for Bcl-x_L was estimated by quantitative comparisons with human Bax (hBax) binding to Bcl-x_L. $InsP_3R$ TM6+C exhibited ∼10-fold greater binding than equivalent amounts of hBax (Fig. 1*D*), suggesting an apparent affinity <50 nM (40, 41). H1 bound to Bcl-x_L with approximately the same affinity as hBax, whereas H4 bound with lower affinity (Fig. 1*D* and Fig. S1*A*). Binding of TM6+C was greater than expected for simple additivity of H1 and H4 binding, suggesting that H1 and H4 contribute synergistically, in agreement with the conclusions from binding competition experiments.

We previously demonstrated that Bcl-x_L binding to the $InsP_3R$ was competitively inhibited by either t-Bid or Bax (27). Bax and t-Bid binding to Bcl-x_L is mediated by their BH3 domains, amphipathic helical regions with a conserved arrangement of a key aspartic acid (Asp) and hydrophobic amino acids (Fig. 2*A*) (23, 42). We speculated that $InsP_3R$ interactions with Bcl-x_L were similarly mediated by BH3-like sequences. Inspection of H1 and H4 revealed conserved BH3-like sequences in both (Fig. 2*A*).

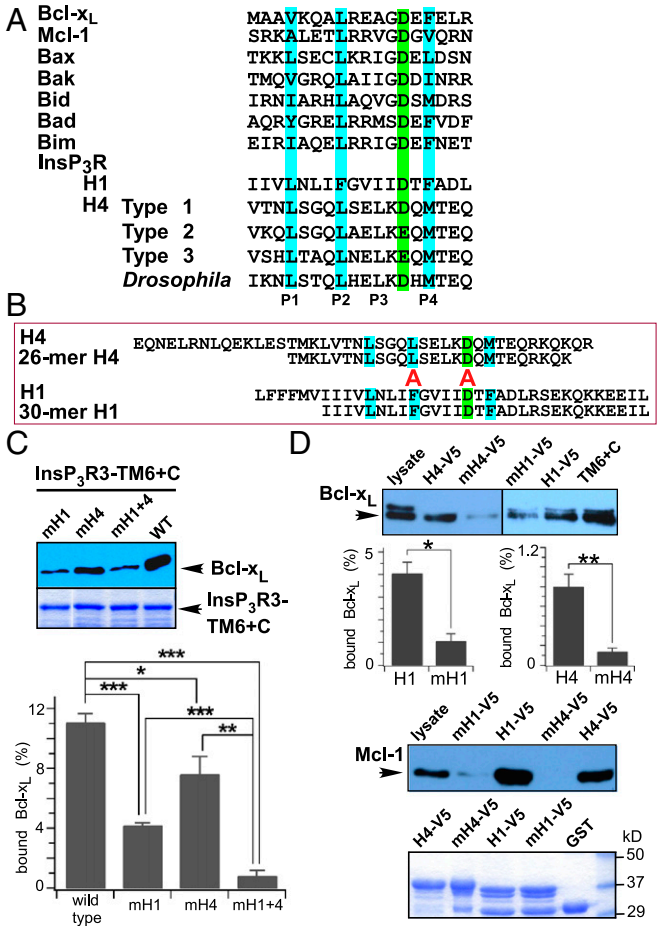

Fig. 2. Bcl-x_L binds to the $InsP_3R$ C terminus by interaction with BH3-like domains. (*A*) Sequence alignment of BH3 domains from Bcl-2 related proteins, with residues critical for binding interactions with other Bcl-2 proteins highlighted. Sequences of short regions within $InsP_3R$ H1 and H4 aligned with Bcl-2 protein BH3 domains. (*B*) Sequence alignments of H4 and H1 with peptides encompassing their respective BH3-like domains. In mutant helices, residues aligned with red "A" were mutated to alanine. (*C*) Pull down of Bcl-x_L by various $InsP_3R3$ TM6+C GST-fusion proteins. Mutations to Ala of residues critical for BH3 domain interactions in either H1 (mH1) or H4 (mH4) inhibit binding of $InsP_3R$ C terminus to Bcl-x_L, with mutations in H1 having most profound effects. (*Lower*) Quantification expressed as percent Bcl-x_L in lysate. Mean ± SEM, $n = 3$; $^*P < 0.05$; $^{**}P < 0.01$; $^{***}P < 0.001$. (*D*) Pull down of Bcl-x_L or Mcl-1 by various $InsP_3R3$ constructs. Mutations in H4 and HI inhibit Bcl-x_L (mean ± SEM, $n = 3$; $^*P < 0.05$; $^{**}P < 0.005$) and Mcl-1 ($n = 3$) binding.

Synthetic H1 and H4 peptides that contained the putative BH3-like domains (Fig. 2*B*) bound to both Bcl-x_L and the anti-apoptotic Bcl-2 protein, Mcl-1, as efficiently as full-length H1 and H4 helices (Fig. S1*B*). Mutations of the key acidic residue and hydrophobic residue at P2 inhibit BH3 domain interactions (42). Mutations to alanine (Ala) of Glu and P2 phenylalanine (Phe) in H1 (mH1) strongly inhibited Bcl-x_L binding to TM6+C (Fig. 2*C*). Similar mutations in H4 (mH4) inhibited binding to a lesser extent (Fig. 2*C*), whereas simultaneous mutations in both H1 and H4 (mH1+4) inhibited binding to an extent observed for mutation in H1 only (Fig. 2*C*), again indicating a higher binding affinity for H1. Similar results were obtained using purified WT and mutant H1 and H4 peptides (Fig. 2*D*). These biochemical results strongly suggest that Bcl-x_L interacts with both H1 and H4 through BH3-like domains contained within each helix in the $InsP_3R$ channel C terminus.

Bcl-x_L Binding to Dual $InsP_3R$ BH3-Like Domains Has Overlapping and Distinct Effects on Channel Gating. To explore the functional consequences of the interaction of Bcl-x_L with the $InsP_3R$, we recorded single $InsP_3R$ channels in native ER membranes by nuclear patch-clamp electrophysiology (1, 27, 43) using chicken DT40 cells with all $InsP_3R$ isoforms genetically deleted (DT40-KO) and engineered to stably express WT or mutant rat type 3 $InsP_3R$ ($InsP_3R3$), the channel isoform that gates most robustly in these cells (32). $InsP_3R3$ activated by suboptimal [$InsP_3$] (1 μM) displayed a low open probability P_o that was elevated by over an order of magnitude by inclusion of 1-μM purified recombinant full-length Bcl-x_L in the pipette solution that bathes the cytoplasmic face of the channel (Fig. 3*A*), in agreement with previous studies (27, 32). The stimulation was dose-dependent, with an apparent K_D of ∼700 nM and Hill coefficient of ∼2 (Fig. 3*A*), suggesting cooperative activation, consistent with Bcl-x_L binding to H1 and H4. Surprisingly, [Bcl-x_L] > ∼2 μM was less effective (Fig. 3*A*). Consequently, the dose-dependence of Bcl-x_L channel activation was biphasic, with half-maximal apparent inhibition observed at ∼3.5 μM with a Hill coefficient >3 (Fig. 3*A*), indicating that apparent inhibition was also a cooperative process possibly reflecting multiple binding sites. To ensure that reduced efficacy of high [Bcl-x_L] to activate channel gating was caused by inhibition mediated by a low-affinity Bcl-x_L binding sites, $InsP_3R$ activity was recorded with higher [$InsP_3$] (3 μM) that is more optimal for channel activity. Addition of 10 μM Bcl-x_L inhibited channel gating under these conditions (Fig. 3*A*), demonstrating that Bcl-x_L both activates and inhibits $InsP_3R$ channel gating, with high-affinity Bcl-x_L binding activating the channel, and Bcl-x_L binding to a low-affinity sites causing channel inhibition. At 1 μM Bcl-x_L, channel activation was caused by an ∼25-fold decrease in the mean closed time. At 10 μM Bcl-x_L, inhibition was caused by a threefold enhancement of the closed time and a twofold decrease in the channel open time (Fig. S2*B*).

Stable cell lines were generated that expressed $InsP_3R3$ with mutations in either H4 (mH4-$InsP_3R3$) or H1 (mH1-$InsP_3R3$) that reduced Bcl-x_L binding to the C terminus (Fig. 2*C*). mH4-$InsP_3R3$ had normal permeation and gating properties and responses to $InsP_3$ (Fig. S2*A*). However, gating activation by Bcl-x_L was completely abolished (Fig. 3*B*). In contrast, high [Bcl-x_L] inhibition was unaffected (Fig. 3*B*). Thus, Bcl-x_L binding to H4 is required for channel activation, whereas inhibition is mediated by Bcl-x_L binding to a different site. Channel gating activation by 1 μM Bcl-x_L was also abolished in mH1-$InsP_3R3$ (Fig. 3*C*). Raising Bcl-x_L to 10 μM still failed to activate the mutant channel (Fig. 3*C*). mH1-$InsP_3R3$ had normal sensitivity to $InsP_3$ (Fig. S2*A*) but had altered conductance and gating properties compared with the WT channel. Single-channel conductance was reduced from 545 pS to 54 ± 6 pS ($n = 4$) for the mutant. Reduced single-channel conductance was caused in part by neutralization of Asp at position 2,590, because a channel with only the D2590 mutation (D2590N-$InsP_3R3$) exhibited reduced conductance (209 ± 3 pS; $n = 11$) (Fig. 3*D*). Altered gating was primarily a consequence of mutating Phe2585, because this residue is predicted to be in close proximity to the channel gate (Fig. 1*A*) (44) and D2590N-$InsP_3R3$ had normal P_o, albeit with reduced open and closed times ($\tau_o \sim \tau_c = 2$ ms) (Fig. 3*D*). To minimize uncertainties associated with a channel with abnormal P_o, we repeated experiments using D2590N-$InsP_3R3$. D2590N-$InsP_3R3$ had normal sensitivity to $InsP_3$ (Fig. S2*A*) but Bcl-x_L failed to activate this mutant channel (Fig. 3*D*). Furthermore, channel-gating inhibition by high [Bcl-x_L] was also abolished (Fig. 3*D*). Taken together, these results indicate that Bcl-x_L binding to both H4 and H1 are required for activation of channel gating, whereas lower affinity Bcl-x_L inhibition requires binding to H1, but not to H4. In agreement, a H4 peptide—but not a mutant peptide mH4—blocked Bcl-x_L channel activation but not

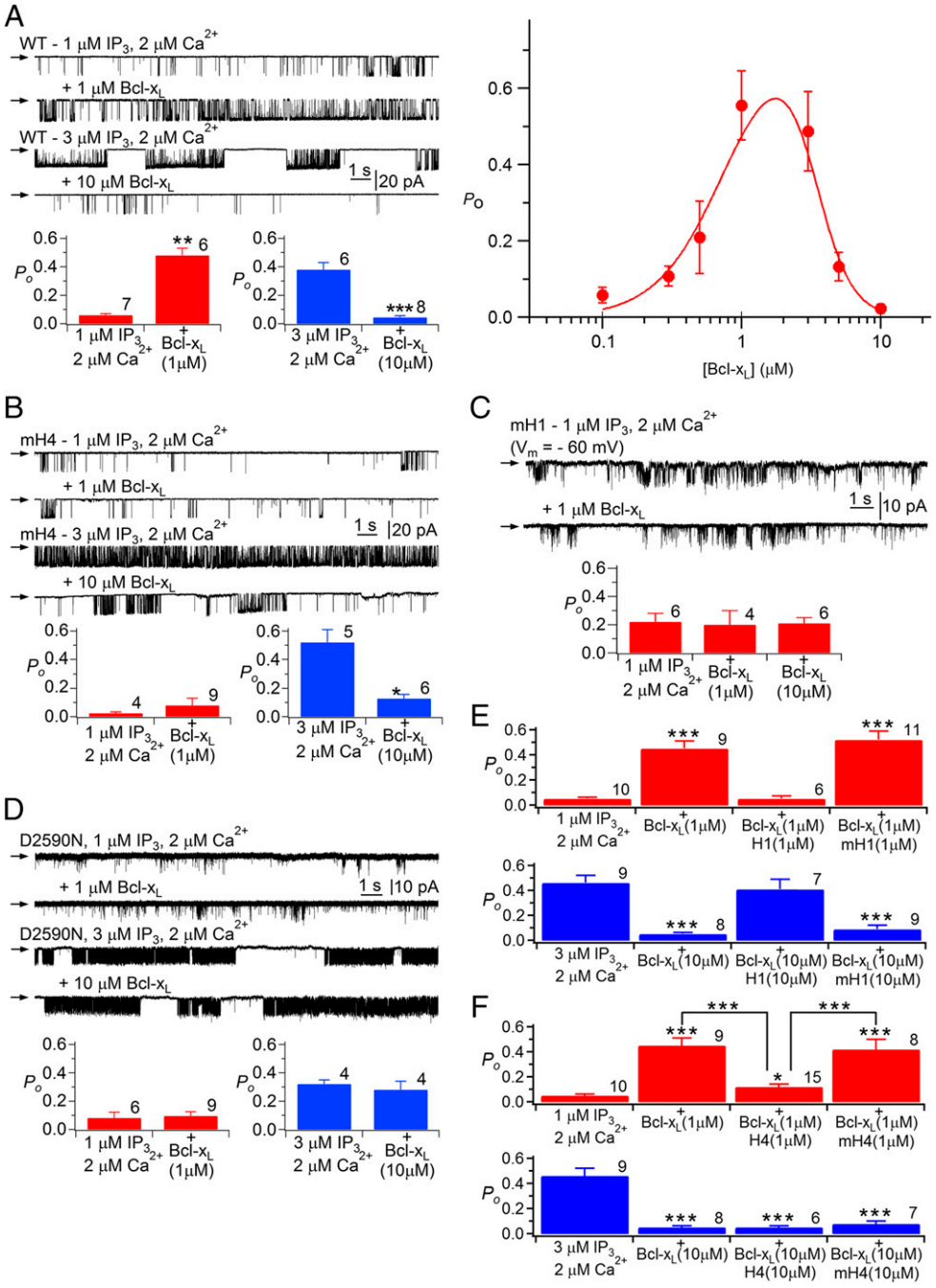

Fig. 3. Bcl-x_L binding to $InsP_3R$ H1 and H4 BH3-like domains regulates channel gating. (*A*, *Left*) $InsP_3R3$ single channel currents with pipette solution containing 1 μM $InsP_3$ and 2 μM free Ca^{2+}, agonist concentrations suboptimal for channel gating. In each trace, arrow indicates zero-current level; openings are downward deflections with pipette voltage = –40 mV. Addition of 1 μM full-length Bcl-x_L activates channel gating (second trace). In the presence of 3 μM $InsP_3$ and 2 μM Ca^{2+}, conditions optimal for channel gating (third trace), 10 μM Bcl-x_L inhibits gating (fourth trace). Histograms summarize activation and inhibition by Bcl-x_L. In all P_o histograms, number of experiments shown above each bar, and shown are mean ± SEM; *$P < 0.05$; **$P < 0.005$; ***$P < 0.001$. (*Right*) Dose-dependence of Bcl-x_L modulation of channel open probability P_o in the presence of 1 μM $InsP_3$ and 2 μM Ca^{2+}. Solid line is from data fitted with a biphasic Hill equation. (*B*) Effects of Bcl-x_L on mH4-$InsP_3R3$ (mH4) stably expressed in DT40-KO cells. (*C*) Effects of Bcl-x_L on mH1-$InsP_3R3$ (mH1) stably expressed in DT40-KO cells. (*D*) Effects of Bcl-x_L on D2590N-$InsP_3R3$ stably expressed in DT40-KO cells. (*E* and *F*) Effects of WT and mutant H1 (*E*) and H4 (*F*) peptides on Bcl-x_L activation and inhibition of $InsP_3R3$ channel activity.

inhibition (Fig. 3*F*), whereas a H1 peptide—but not a mutant mH1—blocked both channel activation and inhibition (Fig. 3*E*).

The BH3 Domain-Binding Pocket in Bcl-x_L Mediates Its Biochemical and Functional Interactions with $InsP_3R$. Bcl-2 protein heterodimerization is mediated by BH3 domain binding to a hydrophobic groove on the surface of its binding partner (23, 42). Key residues in the Bcl-x_L binding pocket that mediate interactions with BH3 domains of Bax and t-Bid include Gly138 and Arg139 (23). The BH3 domain-like sequences in H1 and H4, and the biochemical and functional consequences of mutations in those domains, suggested that the $InsP_3R$ may interact with Bcl-x_L in a manner analogous to proapoptotic Bcl-2 proteins. To explore this theory, we examined biochemical and functional interactions

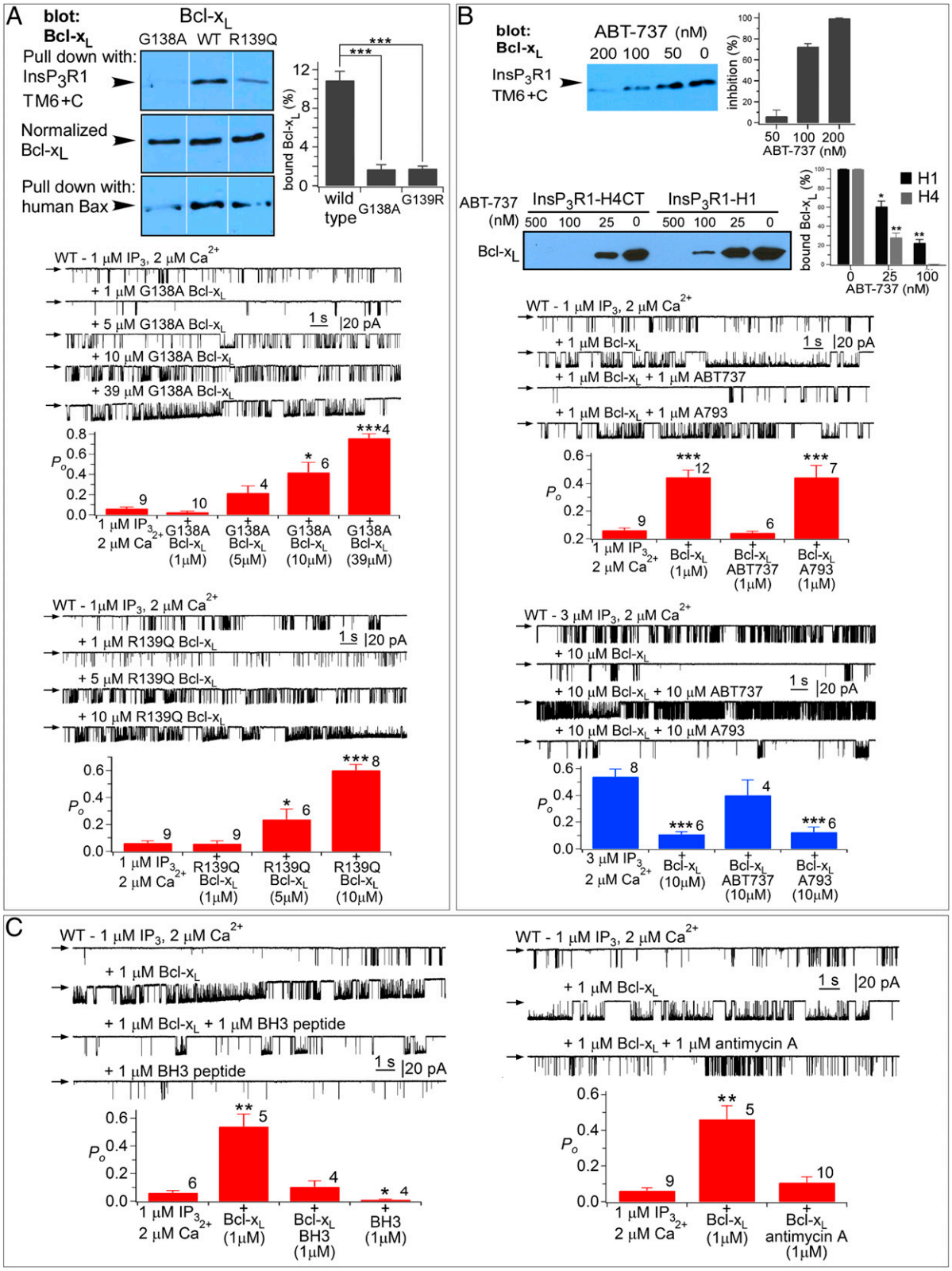

Fig. 4. The BH3 domain-binding pocket in Bcl-x_L mediates its biochemical and functional interaction with the $InsP_3R$ C terminus. (*A*, *Top Left*) Pull down of WT and mutant Bcl-x_L (G138A, R139Q) by Bax and TM6+C GST fusion protein. (*Top Right*) Quantification expressed as percent of Bcl-x_L in lysate. Mean ± SEM, $n = 3$, $^{***}P < 0.001$. (*Middle* and *Lower*) Effects of G138A– and R139Q–Bcl-x_L on $InsP_3R3$ channel activity. In all P_o histograms, number of experiments shown above each bar, and shown are mean ± SEM; $^{*}P < 0.05$; $^{**}P < 0.005$; $^{***}P < 0.001$. (*B*, *Upper* gel, *Left*) Effects of ABT-737 on interaction of Bcl-x_L with WT and mutant TM6+C $InsP_3R$ GST-fusion proteins. (*Upper Right*) Dose-dependent inhibition of Bcl-x_L binding to TM6+C GST fusion protein. Mean ± SEM, $n = 3$; $^{**}P < 0.005$; $^{***}P < 0.001$. (*Lower* gel) Effects of ABT-737 on interaction of Bcl-x_L with $InsP_3R$ GST-H1 peptide and GST-H4 peptide that contained H4 extending to the C terminus. (*Right*) Quantification, mean ± SEM, $n = 3$; $^{*}P < 0.05$; $^{**}P < 0.005$. (*Lower*) Effects of ABT-737 and its inactive enantiomer A-793844 (A793) on $InsP_3R3$ channel gating. (*C*) Effects of Bax BH3 peptide (*Left*) and antimycin-A (*Right*) on $InsP_3R3$ channel gating.

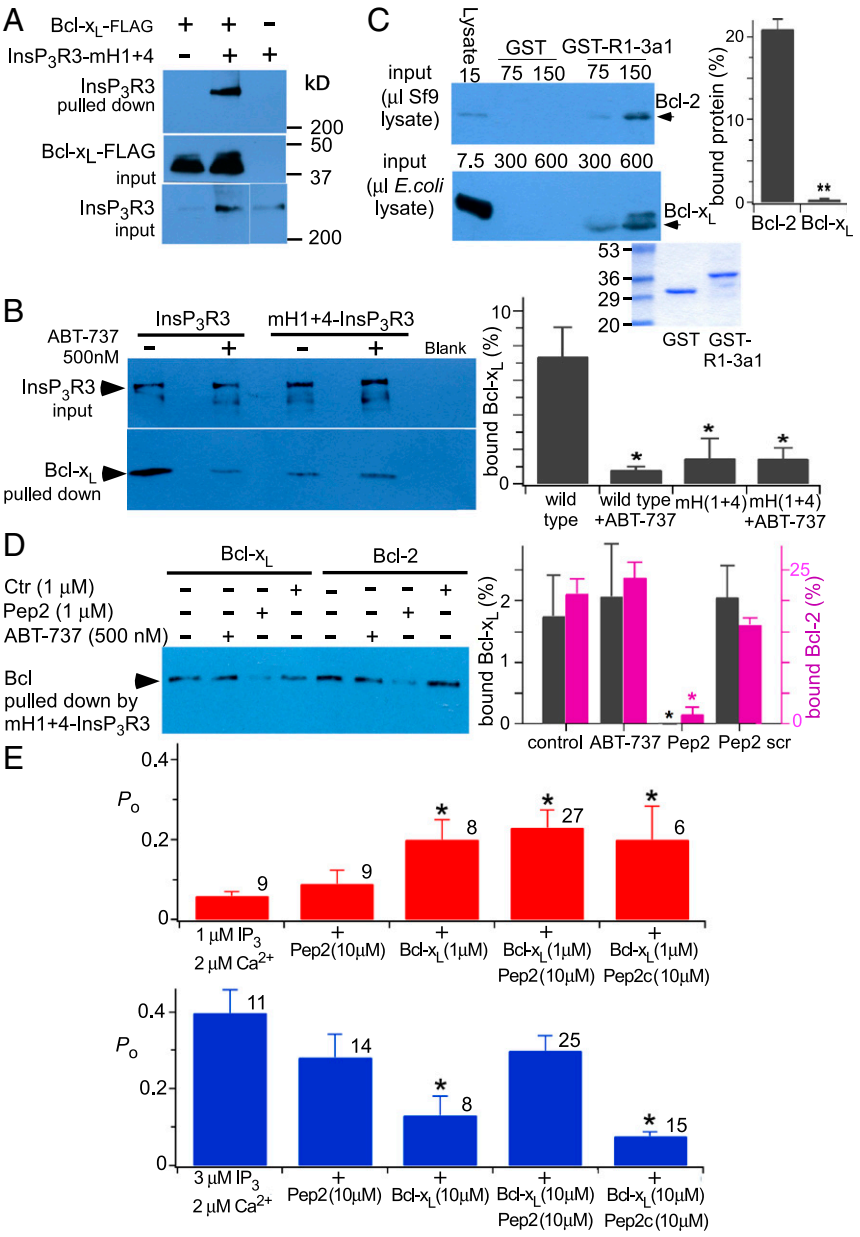

Fig. 5. Additional determinants in $InsP_3R$ mediate biochemical and functional interactions with Bcl-x_L. (*A*) Interaction of full-length mH1+H4-$InsP_3R3$ with FLAG-tagged Bcl-x_L (*Top*). Flag-tagged Bcl-x_L on antibody beads (*Middle*) and mH1+H4-$InsP_3R3$ in lysate (*Bottom*) shown. (*B*, *Left*) Effects of ABT-737 on pull down of Bcl-x_L (*Lower*) by $InsP_3R3$ and mH1+H4-$InsP_3R3$ (*Upper*) stably expressed in DT40-KO cells and bound to a GST-CaBP1 column. (*Right*) Quantification of Bcl-x_L pulled down as percent in lysate. Mean ± SEM, $n = 3$; $^*P < 0.05$. (*C*) Purified rat Bcl-2 (*Top*) and Bcl-x_L (*Middle*) binding to $InsP_3R1$ GST-3a1 peptide. Coomassie blue staining (*Bottom*) shows GST fusion protein equivalence. (*Right*) Quantification of protein pulled down as percent in lysate using 75 µL Bcl-2 and 300 µL Bcl-x_L. Mean ± SEM, $n = 3$; $^{**}P < 0.005$. (*D*, *Left*) Pull down of mH1+H4-$InsP_3R3$ stably expressed in DT40-KO cells by FLAG-tagged Bcl-x_L and Bcl-2 in the presence or absence of ABT-737, Pep2, or a scrambled peptide (Ctr). (*Right*) Quantification of Bcl-x_L and Bcl-2 pulled down as percent in lysate. Mean ± SEM, $n = 3$; $^*P < 0.05$. (*E*) Summary of $InsP_3R3$ channel P_o recorded with pipette solution containing $InsP_3$, free Ca^{2+}, Pep2 peptide, Pep2c scrambled peptide, or Bcl-x_L, as indicated. Number of experiments shown above each bar; mean ± SEM; $^*P < 0.05$ relative to control values (first bar of charts).

of the $InsP_3R$ with purified full-length Bcl-x_L proteins with either Gly138 or Arg139 mutated. As a control, we verified that G138A–Bcl-x_L binding to hBax was significantly reduced compared with WT Bcl-x_L (Fig. 4*A*). Binding of G138A–Bcl-x_L to TM6+C was profoundly inhibited compared with WT Bcl-x_L (Fig. 4*A*) ($P < 0.001$), because of reduced binding at both H1 and H4 (Fig. S3). The weakened biochemical interactions were manifested as significantly reduced potencies at the single-channel level. Whereas 1 µM WT Bcl-x_L activated the channel gating robustly, 1 µM G138A–Bcl-x_L was without effect (Fig. 4*A*). However, higher concentrations activated gating (Fig. 4*A*) ($P < 0.001$), indicating that the G138A mutation significantly reduced the binding affinity, consistent with the biochemical data. Similar data were obtained with R139Q–Bcl-x_L (Fig. 4*A*). These results suggest that the pocket that binds to BH3 domains of Bcl-2 family proteins also mediates biochemical and functional interactions of Bcl-x_L with BH3-like domains in $InsP_3R$. To test this further, we examined the effects of ABT-737, a small molecule that binds specifically in the Bcl-x_L surface groove and prevents Bax and t-Bid binding (45). ABT-737 inhibited the interaction of TM6+C with Bcl-x_L with half-maximal concentration <100 nM (Fig. 4*B*). Bcl-x_L binding to H1 was less sensitive to ABT-737 than was H4

(Fig. 4*B*), consistent again with higher-affinity Bcl-x_L binding to H1. ABT-737 (1 μM), but not inactive enantiomer, completely blocked channel activation by Bcl-x_L (Fig. 4*B*). Furthermore, ABT-737 also completely blocked high [Bcl-x_L] inhibition of channel gating (Fig. 4*B*). Other pharmacological agents that disrupt Bcl-x_L–BH3 domain interactions also blocked effects of Bcl-x_L on $InsP_3R$ channel gating, including a synthetic Bax BH3 domain peptide and antimycin A (46) (Fig. 4*C*). Together, these results implicate the BH3 binding groove in Bcl-x_L in its biochemical and functional interactions with the $InsP_3R$.

Additional Determinants in $InsP_3R$ Mediate Biochemical and Functional Interactions with Bcl-x_L. $InsP_3R$ channel activation by Bcl-x_L requires binding to both H1 and H4 BH3-like domains, whereas channel inhibition by high Bcl-x_L concentrations requires binding to H1 but H4 is not required. Low-affinity channel inhibition mediated by H1 is in apparent conflict with high-affinity biochemical binding of H1 to Bcl-x_L (Fig. 1). This finding suggested that low-affinity inhibition of channel gating may involve determinants in addition to the H1 BH3-like domain. Indeed, Bcl-x_L bound weakly to full-length $InsP_3R$ with both H1 and H4 mutated (Fig. 5 *A* and *B*) that was insensitive to ABT-737 (500 nM) (Fig. 5*B*). Bcl-2 interacts with a region in the $InsP_3R$ coupling domain encompassing residues 1,347–1,426, referred to as 3a1 (37). Bcl-x_L bound to GST-3a1, but by comparison with Bcl-2, its binding was very much weaker (Fig. 5*C*). Binding of Bcl-2 as well as residual binding of Bcl-x_L to mH1+4-$InsP_3R3$, although insensitive to ABT-737, were similarly inhibited by a peptide (Pep2; P2 in ref. 37) encompassing these residues (Fig. 5*D*). Bcl-x_L binding to the C terminus both activates and inhibits $InsP_3R$ channel activity (Fig. 3), whereas only inhibition of Ca^{2+} release has been reported for the interaction of Bcl-2 with the channel (17). We hypothesized that if this region contributed additional binding determinants required for H1-mediated inhibition of channel gating, inclusion of Pep2 in the patch pipette solution would inhibit high [Bcl-x_L] inhibition of channel gating. Neither the peptide itself (10 μM) nor a scrambled control peptide had effects on channel gating in the absence of Bcl-x_L, nor did either peptide affect 1 μM Bcl-x_L activation (Fig. 5*E*). In contrast, the peptide completely blocked the inhibitory effects of 10 μM Bcl-x_L (Fig. 5*E*). These results demonstrate that channel-gating inhibition by high [Bcl-x_L] requires binding to both the H1 BH3-like domain and a region (3a1) localized in the channel-coupling domain. The BH4 domain of Bcl-2 has been implicated in its binding to the $InsP_3R$ (35, 36). It is possible that the BH4 domain of Bcl-x_L also interacts with this channel region, because a synthetic Bcl-x_L BH4 peptide reduced high [Bcl-x_L]-mediated channel inhibition (Fig. S4).

$InsP_3R$ BH3-Like Domains Regulate Cell Viability. It was shown previously that Bcl-x_L interaction with the $InsP_3R$ conferred apoptosis protection (27, 32), likely by stimulating low-level Ca^{2+} signaling that adapts cells to be resistant to stress (31). Based on the results above, we hypothesized that Bcl-x_L binding to $InsP_3R$ C-terminal BH3-like domains mediates this protection. To test this theory, stable DT40-KO cells expressing human Bcl-x_L (27) were engineered to express WT $InsP_3R3$ or mH4-$InsP_3R3$ at equivalent levels and used in cell viability assays. Because of its altered conductance and gating properties, mH1-$InsP_3R3$ was considered inappropriate in these assays. Cell death was triggered by 500 nM staurosporine (STS) in clonal lines that expressed comparable levels of Bcl-x_L and WT vs. mutant $InsP_3R$. With mH4-$InsP_3R3$ and $InsP_3R3$ expressed at levels comparable to WT cells (low expressers), STS induced cell death in both lines, but the mH4-$InsP_3R3$ cells were more sensitive (Fig. 6*A*). We also examined cells in which the WT and mutant $InsP_3R$ were overexpressed by >50-fold compared with normal (Fig. 6*A* and Fig. S5). With much higher levels of $InsP_3R$ expression, Bcl-x_L stimulation of channel gating may contribute to excessive Ca^{2+} release to promote cell death. In this case, preventing Bcl-x_L activation of $InsP_3R$ would be predicted to confer protection. In agreement, cell death was enhanced with increasing levels of strong overexpression of $InsP_3R3$ (Fig. 6*A*). Importantly, mutation of the channel H4 BH3-like domain conferred significant protection in cells expressing very high levels of $InsP_3R$ (Fig. 6*A*).

To further explore the roles of Bcl-x_L interaction with the channel H1 and H4 domains, we generated TAT fusion proteins of H1 and H4 peptides to facilitate their delivery into cells. Here, we reasoned that blocking the Bcl-x_L–$InsP_3R$ interaction by peptide competition would reveal a role of these domains in normal cell viability. Neither H4-TAT (1 μM) nor the control peptides (scrambled H4 sequence) affected single $InsP_3R$ channel activity, whereas H4-TAT completely blocked activation by 1 μM Bcl-x_L (Fig. 6*B*), validating use of the peptides for cellular studies. Exposure of DT40 cells for 24 h to up to 4 μM TAT-H1 or TAT-H4 was without effect on cell viability (Fig. 6*C*). In contrast, combined exposure to both TAT-H1 and TAT-H4 caused a dose-dependent loss of cell viability, with nearly complete cell killing at 4 μM (Fig. 6*C*). In addition, although exposure to 1–5 μM TAT-H4 had no effect on viability, it strongly potentiated killing induced by 500 nM STS (Fig. 6*C*). Similarly, simultaneous exposure to TAT-H1 and TAT-H4 peptides caused profound killing of human Raji lymphoblasts and MCF7 breast cells, whereas control peptides (scrambled H1 and H4 sequences) were without effect (Fig. 6*D*). By flow cytometry analyses, cell death appeared to be distinct from apoptosis induced by STS, suggesting necrosis as the primary mechanism. TOTO-3 staining also suggested that necrosis was the major mechanism of cell death (Fig. 6*D*). Taken together, these results suggest that the interaction between Bcl-x_L and the H1/H4 domains of the $InsP_3R$ plays an important role in regulating cell viability.

Discussion

Antiapoptotic Bcl-2 family proteins Bcl-x_L, Bcl-2, and Mcl-1 bind to the $InsP_3R$ Ca^{2+} release channel C terminus, enhancing its channel activity and Ca^{2+} release that affords ER-based apoptosis protection (27, 31, 32). Bcl-x_L interacts with the C terminus as strongly as with the full-length channel, suggesting that the C terminus represents the major binding determinant for Bcl-x_L (27) and possibly the other antiapoptotic Bcl-2 proteins. Here, using biochemical approaches and single-channel electrophysiology, we have defined two distinct sites in the C terminus that mediate channel interactions with Bcl-x_L. Furthermore, we defined determinants in Bcl-x_L that mediate its interactions with both sites. Remarkably, the interactions are highly analogous to the interactions of proapoptotic Bcl-2 family proteins with Bcl-x_L. Thus, we have identified two BH3-like domains in the $InsP_3R$ C terminus that interact with different affinities with the hydrophobic surface groove of Bcl-x_L that binds BH3 domains in apoptotic proteins. Importantly, the biochemical results are strongly supported by electrophysiological analyses of the effects of WT and mutant Bcl-x_L on the activities of single WT and mutant $InsP_3R$ channels. Interaction of Bcl-x_L with the two sites has distinct functional effects, activating and inhibitory, which result in a biphasic concentration dependence of the effects of Bcl-x_L on channel gating. Cell viability was compromised by interfering with the interactions, highlighting their importance. Of note, we found that a third binding site in the coupling domain, previously shown to interact with Bcl-2, participated in the inhibitory effects on channel gating of Bcl-x_L binding to the C terminus, thereby providing a unifying framework for understanding the biochemical and functional interactions of antiapoptotic Bcl-2 family proteins with the $InsP_3R$.

Various lines of evidence suggest that two regions in the $InsP_3R$ C terminus interact with Bcl-x_L and that both are BH3 domain-like. First, the sequences of the interacting regions are reminiscent of BH3 domains. H1 and H4 have arrangements of

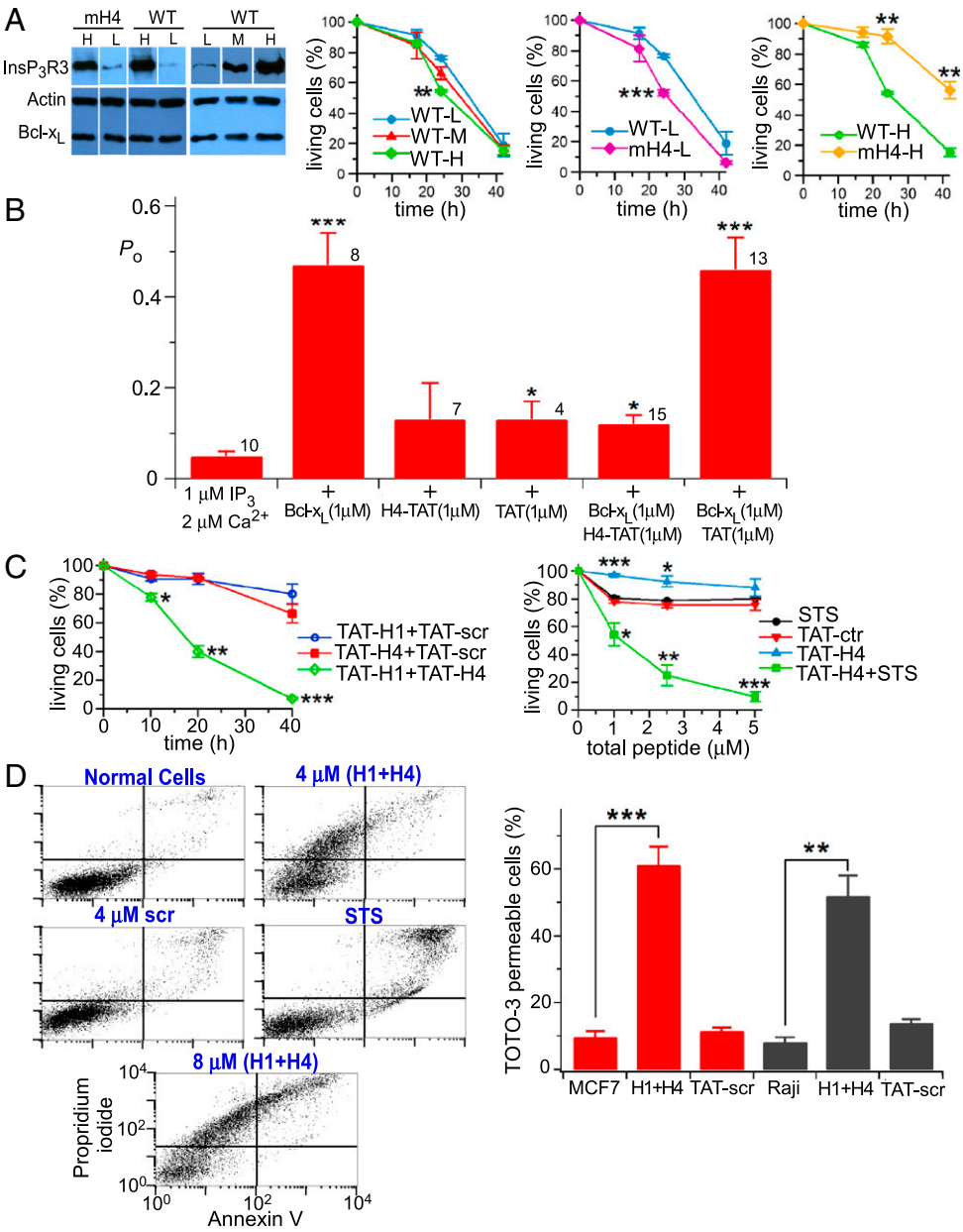

Fig. 6. $InsP_3R$ BH3-like domains regulate cell viability. (*A*) Expression levels of WT and mH4 (mH4)-$InsP_3R3$ and Bcl-x_L in DT40 cells used in viability assays in response to 500 nM STS. (*Left* time course) Viability (TOTO-3 uptake) of cells with different WT $InsP_3R3$ expression levels. (*Center* time course) Responses of cells expressing WT and mH4-$InsP_3R3$ at low levels. (*Right* time course) Responses of cells expressing WT and mH4-$InsP_3R3$ at high levels. $n = 3$ experiments. Mean ± SEM; $^{**}P < 0.005$; $^{***}P < 0.001$. (*B*) Summary of $InsP_3R3$ P_o activated by 1 μM $InsP_3$ in presence of 2 μM Ca^{2+} in response to Bcl-x_L and H4-TAT and control scrambled TAT peptides, as indicated. Number of patches indicated; Mean ± SEM; $^{*}P < 0.05$, $^{***}P < 0.001$. (*C*) Cell viability (TOTO-3 uptake) of WT DT40 cells treated with STS (500 nM) or TAT fusion peptides for 24 h. (*Left*) 2 μM of each peptide was used. $n = 3$ experiments. Mean ± SEM; $^{*}P < 0.05$; $^{**}P < 0.005$; $^{***}P < 0.001$ compared with control scrambled TAT peptide. (*D*, *Left*) Effects of H1- and H4-TAT peptides, STS (500 nM) and scrambled TAT fusion peptides on human Raji cell viability by flow cytometry. (*Right*) Cell necrosis (TOTO-3 permeability) of MCF7 and Raji cells treated or not with 2 μM TAT-H1 plus 2 μM TAT-H4 peptides (H1+H4) or 4 μM scrambled TAT peptides (TAT-scr).

critical negatively changed and surrounding hydrophobic residues that are present in all BH3 domains (42). In the high-affinity H1 helix, the negatively charged residue is Asp, as in bone fide BH3 domains. In H4, it is Asp in the type 1 and *Drosophila* $InsP_3Rs$, and Glu in types 2 and 3 $InsP_3R$, which preserve the critical negative charge. The hydrophobic Leu at the P2 position is conserved, except in H1, where it is hydrophobic Phe. A notable difference in the sequence of the BH3-like domains in H1 and H4 is the absence of Gly immediately preceding the Asp. In H1 it is Ile and in H4 a Lys. Both residues are bulkier than Gly, the Lys introduces a charge, and both might be expected to diminish the binding affinity to Bcl-x_L. Nevertheless, H1 bound to Bcl-x_L with a higher apparent affinity than the Bax BH3 domain, suggesting that Ile in lieu of Gly is well accommodated by Bcl-x_L. Lys in H4 is bulkier than Ile, which together with its charge, may account for the lower apparent affinity of H4. In agreement, mutation of Lys to Gly strongly enhanced the binding of H4 to Bcl-x_L (Fig. S6). Nevertheless, mutagenesis of the key Asp and hydrophobic P2 residue strongly inhibited binding of both helices to Bcl-x_L. In addition, mutation of Arg139 in Bcl-x_L, which interacts

with the BH3 Asp, as well as Gly138, which also contributes to the binding interaction with BH3 domains, significantly reduced binding of each $InsP_3R$ helix with Bcl-x_L. Finally, the biochemical interaction of the C terminus and each helix was strongly inhibited by ABT-737 and the Bax BH3 domain peptide, both of which bind specifically in the Bcl-x_L surface groove. The biochemical data therefore strongly support the conclusion that interaction of Bcl-x_L with the $InsP_3R$ is mediated by both H1 and H4 with the surface pocket in Bcl-x_L in a manner that is highly reminiscent of the interactions of Bcl-x_L with proapoptotic BH3 domains. Despite a similar strategy among Bcl-2 family proteins of BH3 domain binding to a surface hydrophobic groove, there is a high degree of specificity in the interactions (42, 47). Furthermore, the binding pockets of some Bcl-2 family members, including Bcl-x_L, have considerable conformational flexibility to accommodate different BH3 domains (48, 49). Such structural flexibility may explain the interaction with the BH3-like domains in the $InsP_3R$.

Unique to the study of Bcl-2 protein interactions, real-time single molecule recordings here validated the conclusions reached from biochemical studies, and provided insights into the functional implications of the interaction of Bcl-x_L with the $InsP_3R$. Using WT and mutant proteins and single-channel electrophysiology, we found a remarkable concordance between the biochemical and electrophysiological results. First, Bcl-x_L both activated and inhibited the channel, suggesting that it interacts with the channel in at least two functional sites. High-affinity channel gating activation requires Bcl-x_L binding to both H1 and H4, in agreement with the biochemical demonstration that the entire C terminus had the highest affinity for Bcl-x_L. In contrast, low-affinity channel inhibition required binding to only the H1 helix. Thus, the biochemistry and electrophysiology suggest that H1 and H4 are both involved in the interactions of Bcl-x_L with the $InsP_3R$, with functional consequences. The single-channel recordings also provide strong support for the conclusion that the interactions of each helix are mediated by canonical BH3 domain interactions with the surface groove in Bcl-x_L. Mutation of either Gly138 or Arg139 in the Bcl-x_L binding pocket strongly reduced the ability of Bcl-x_L to activate channel gating. Normal channel activation by the mutant Bcl-x_L proteins was achieved when [Bcl-x_L] was raised by 10- to 40-fold. It is likely that the lower-affinity inhibitory site interaction was similarly affected by these mutations, but they were not observed because Bcl-x_L could not be used in high-enough concentrations. This conclusion is supported by the effects of ABT-737, antimycin C, and the Bax BH3 domain peptide. All bind in the hydrophobic pocket in Bcl-x_L and inhibited both channel activation and inhibition by Bcl-x_L. In summary, single-channel electrophysiology provides strong validation of the biochemical studies. The studies demonstrate that the biochemical interactions have strong functional implications, and they support a model in which Bcl-x_L interacts with two BH3-like domains in the channel C terminus.

After these experiments were completed, a high-resolution cryo-electron microscopy (cryo-EM) structure of rat $InsP_3R1$ was solved (44). The structure demonstrates that the TM6 helix extends into the cytoplasm, defining what we have referred to as H1. The side-chain of D2590 (2591 in the structure) points toward the cytoplasmic vestibule of the permeation pathway, in agreement with our studies that showed that neutralization of this residue reduced channel conductance, suggesting that D2590 contributes to the electrostatic environment in the cytoplasmic vestibule that promotes cation conduction. In the structure, F2585 (2586 in the structure) appears to form the channel gate. It is not obvious how Bcl-x_L could access this site. However, the channel structure was solved in the absence of $InsP_3$ and Ca^{2+}, and in a closed conformation whose relevance for the structure of an active liganded channel remains to be determined. Bcl-x_L interaction with this region in an active channel suggests that the channel cytoplasmic vestibule must become more accessible during channel gating than is evident in the cryo-EM structure. Nevertheless, interaction with such a critical site in the channel would be predicted to influence channel gating, as we observe.

H4 is referred to as the C-terminal domain (CTD) in the cryo-EM structure (44). It is an extended α-helix that has contacts with the $InsP_3$ binding domain and a ring of helical linker (LNK) domains, forming a connection between the $InsP_3$ binding domain and TM6. The LNK domain contains the two helices we referred to here as H2 and H3. The Bcl-x_L binding determinants we defined here are located immediately proximal to the major LNK-interacting CTD residues. The CTD is in an ideal position to transmit conformational changes associated with Bcl-x_L binding to both the $InsP_3$-binding domain and the channel-gating machinery, and may therefore provide a structural basis for the role of H4 binding in Bcl-x_L sensitization of the channel to $InsP_3$ (27) and in channel-gating activation. Nevertheless, our results indicate that simultaneous Bcl-x_L binding to the H1 region is also required for channel activation, suggesting a model in which conformational changes in the CTD induced by Bcl-x_L binding to H4 are transmitted to the channel regions that destabilize channel closed states only when Bcl-x_L is simultaneously bound to TM6.

High [Bcl-x_L] inhibition of channel gating was independent of the CTD. Inhibition of $InsP_3R$-mediated Ca^{2+} release has been observed as a functional effect of Bcl-2 interaction with the channel (17). There, the interaction determinants described are different from those defined here. The Bcl-2 BH4 domain, a helix localized on the opposite face of the protein from the surface groove, interacts with a 3a1 region in the coupling domain (35, 37). We found residual binding of Bcl-x_L to the channel after elimination of its binding to the C terminus, which was localized to the same 3a1 region. Although the affinity for Bcl-x_L was much lower than that for Bcl-2, the interaction nevertheless appears to be critical for channel-gating inhibition by high [Bcl-x_L] because a peptide that blocks the (residual) interaction of both Bcl-2 and Bcl-x_L blocked the ability of Bcl-x_L to inhibit channel gating. Thus, high-affinity Bcl-x_L binding to H1 and simultaneous low-affinity interaction with 3a1 accounts for channel-gating inhibition by high [Bcl-x_L]. Our results suggest a unifying framework that rationalizes previously discrepant results regarding the biochemical and functional implications of different antiapoptotic Bcl-2 family protein interactions with the $InsP_3R$. It will be of interest to determine if inhibition of $InsP_3R$-mediated Ca^{2+} release by Bcl-2 requires its simultaneous binding to H1. Channel activation requires at least two Bcl-x_L molecules to interact with a tetrameric $InsP_3R$ channel, because the interactions involve two sites (H1, H4) with the same binding site on Bcl-x_L. In contrast, a single Bcl-x_L molecule could possibly mediate channel inhibition, by binding H1 with its surface groove and 3a1 with another part of the molecule, perhaps the BH4 domain on the opposite surface.

The biphasic concentration dependence of effects of Bcl-x_L on channel gating suggests that functional effects in cells will vary with expression levels and physical proximity of Bcl-x_L and the $InsP_3R$. A priori it might be expected that the high-affinity, activating effects of Bcl-x_L will usually dominate. Because low-level constitutive $InsP_3R$-mediated Ca^{2+} release is essential for preserving normal bioenergetics under basal conditions (8), we expected that the interaction of Bcl-x_L with H1 and H4 would provide resistance to stress and promote cell viability. With $InsP_3R$ expressed at approximately normal levels, intact H1 and H4 BH3-like domains play important roles in cell viability. In contrast, when $InsP_3R$ is grossly overexpressed, the domains sensitize cells to stress, possibly because of excessive Ca^{2+} release that activates death pathways. Both results suggest that H1 and H4 play important roles in regulating the level of channel activity

in vivo, and they indicate that antiapoptotic Bcl-2 protein $InsP_3R$ C-terminal interactions play important roles in regulating the channels under normal conditions in the cell types examined.

In summary, we have identified unique molecular interactions of Bcl-x_L with the $InsP_3R$ that involves dual BH3-like domains in the C terminus of the channel. The interactions of the surface hydrophobic groove of Bcl-x_L with these domains have both activating and inhibitory effects on channel gating. These interactions are important in regulating channel activity in vivo in a manner that strongly influences sensitivity to cell stress and cell viability. Because drugs such as ABT-737 that target BH3–Bcl-2 family protein interactions are being developed as cancer therapeutics, our results suggest an additional target, the interaction of Bcl-2 proteins with the $InsP_3R$, that may influence their efficacy. Furthermore, ABT-737 inhibition of enhanced $InsP_3R$-mediated Ca^{2+} release in diabetic vascular smooth muscle cells (50) may suggest that this interaction could be targeted for other diseases as well.

Materials and Methods

Details regarding the sources of materials used, cell culture and generation of cell lines, plasmid construction and virus generation, protein and peptide expression, synthesis and purification, the sequences of peptides used, details regarding GST-fusion protein pull downs, fluorescence binding and Western blotting assays, cell viability assays, single-channel electrophysiology, and analyses and statistics are discussed in *SI Materials and Methods*.

ACKNOWLEDGMENTS. We thank Dr. Chi Li for reagents and advice, and Dr. King-Ho Cheung and Ms. Lijuan Mei for technical assistance. This study was supported by National Institutes of Health Grant GM56328 (to J.K.F.) and Shanghai Institute of Planned Parenthood Research Grant PD2012-4 (to J.Y.).

1. Foskett JK, White C, Cheung KH, Mak D-OD (2007) Inositol trisphosphate receptor Ca^{2+} release channels. *Physiol Rev* 87(2):593–658.
2. de Brito OM, Scorrano L (2010) An intimate liaison: Spatial organization of the endoplasmic reticulum-mitochondria relationship. *EMBO J* 29(16):2715–2723.
3. Naon D, Scorrano L (2014) At the right distance: ER-mitochondria juxtaposition in cell life and death. *Biochim Biophys Acta* 1843(10):2184–2194.
4. Hajnóczky G, Robb-Gaspers LD, Seitz MB, Thomas AP (1995) Decoding of cytosolic calcium oscillations in the mitochondria. *Cell* 82(3):415–424.
5. Jouaville LS, Pinton P, Bastianutto C, Rutter GA, Rizzuto R (1999) Regulation of mitochondrial ATP synthesis by calcium: Evidence for a long-term metabolic priming. *Proc Natl Acad Sci USA* 96(24):13807–13812.
6. Duchen MR (2000) Mitochondria and calcium: From cell signalling to cell death. *J Physiol* 529(Pt 1):57–68.
7. Luzzi V, Sims CE, Soughayer JS, Allbritton NL (1998) The physiologic concentration of inositol 1,4,5-trisphosphate in the oocytes of *Xenopus laevis*. *J Biol Chem* 273(44): 28657–28662.
8. Cárdenas C, et al. (2010) Essential regulation of cell bioenergetics by constitutive $InsP_3$ receptor Ca^{2+} transfer to mitochondria. *Cell* 142(2):270–283.
9. Smith IF, Shuai J, Parker I (2011) Active generation and propagation of Ca^{2+} signals within tunneling membrane nanotubes. *Biophys J* 100(8):L37–L39.
10. Ju YK, Woodcock EA, Allen DG, Cannell MB (2012) Inositol 1,4,5-trisphosphate receptors and pacemaker rhythms. *J Mol Cell Cardiol* 53(3):375–381.
11. Szalai G, Krishnamurthy R, Hajnóczky G (1999) Apoptosis driven by IP(3)-linked mitochondrial calcium signals. *EMBO J* 18(22):6349–6361.
12. Bernardi P (1999) Mitochondrial transport of cations: Channels, exchangers, and permeability transition. *Physiol Rev* 79(4):1127–1155.
13. Orrenius S, Gogvadze V, Zhivotovsky B (2015) Calcium and mitochondria in the regulation of cell death. *Biochem Biophys Res Commun* 460(1):72–81.
14. Pinton P, et al. (2001) The Ca^{2+} concentration of the endoplasmic reticulum is a key determinant of ceramide-induced apoptosis: Significance for the molecular mechanism of Bcl-2 action. *EMBO J* 20(11):2690–2701.
15. Scorrano L, et al. (2003) BAX and BAK regulation of endoplasmic reticulum Ca^{2+}: A control point for apoptosis. *Science* 300(5616):135–139.
16. Oakes SA, Opferman JT, Pozzan T, Korsmeyer SJ, Scorrano L (2003) Regulation of endoplasmic reticulum Ca^{2+} dynamics by proapoptotic BCL-2 family members. *Biochem Pharmacol* 66(8):1335–1340.
17. Greenberg EF, Lavik AR, Distelhorst CW (2014) Bcl-2 regulation of the inositol 1,4,5-trisphosphate receptor and calcium signaling in normal and malignant lymphocytes: Potential new target for cancer treatment. *Biochim Biophys Acta* 1843(10):2205–2210.
18. Zhong F, et al. (2011) Induction of Ca^{2}+-driven apoptosis in chronic lymphocytic leukemia cells by peptide-mediated disruption of Bcl-2-IP3 receptor interaction. *Blood* 117(10):2924–2934.
19. Boehning D, et al. (2003) Cytochrome c binds to inositol (1,4,5) trisphosphate receptors, amplifying calcium-dependent apoptosis. *Nat Cell Biol* 5(12):1051–1061.
20. Ferrari D, et al. (2002) Endoplasmic reticulum, Bcl-2 and Ca^{2+} handling in apoptosis. *Cell Calcium* 32(5-6):413–420.
21. Rizzuto R, et al. (2003) Calcium and apoptosis: Facts and hypotheses. *Oncogene* 22(53):8619–8627.
22. Delbridge AR, Strasser A (2015) The BCL-2 protein family, BH3-mimetics and cancer therapy. *Cell Death Differ* 22(7):1071–1080.
23. Petros AM, Olejniczak ET, Fesik SW (2004) Structural biology of the Bcl-2 family of proteins. *Biochim Biophys Acta* 1644(2-3):83–94.
24. Germain M, Shore GC (2003) Cellular distribution of Bcl-2 family proteins. *Sci STKE* 2003(173):pe10.
25. Szegezdi E, Macdonald DC, Ní Chonghaile T, Gupta S, Samali A (2009) Bcl-2 family on guard at the ER. *Am J Physiol Cell Physiol* 296(5):C941–C953.
26. Chen R, et al. (2004) Bcl-2 functionally interacts with inositol 1,4,5-trisphosphate receptors to regulate calcium release from the ER in response to inositol 1,4,5-trisphosphate. *J Cell Biol* 166(2):193–203.
27. White C, et al. (2005) The endoplasmic reticulum gateway to apoptosis by Bcl-$X_{(L)}$ modulation of the $InsP_3R$. *Nat Cell Biol* 7(10):1021–1028.
28. Bonneau B, et al. (2014) The Bcl-2 homolog Nrz inhibits binding of IP3 to its receptor to control calcium signaling during zebrafish epiboly. *Sci Signal* 7(312):ra14.
29. Schulman JJ, Wright FA, Kaufmann T, Wojcikiewicz RJ (2013) The Bcl-2 protein family member Bok binds to the coupling domain of inositol 1,4,5-trisphosphate receptors and protects them from proteolytic cleavage. *J Biol Chem* 288(35):25340–25349.
30. Hanson CJ, Bootman MD, Distelhorst CW, Wojcikiewicz RJ, Roderick HL (2008) Bcl-2 suppresses Ca^{2+} release through inositol 1,4,5-trisphosphate receptors and inhibits Ca^{2+} uptake by mitochondria without affecting ER calcium store content. *Cell Calcium* 44(3):324–338.
31. Eckenrode EF, Yang J, Velmurugan GV, Foskett JK, White C (2010) Apoptosis protection by Mcl-1 and Bcl-2 modulation of inositol 1,4,5-trisphosphate receptor-dependent Ca^{2+} signaling. *J Biol Chem* 285(18):13678–13684.
32. Li C, et al. (2007) Apoptosis regulation by Bcl-x(L) modulation of mammalian inositol 1,4,5-trisphosphate receptor channel isoform gating. *Proc Natl Acad Sci USA* 104(30): 12565–12570.
33. Lewis A, Hayashi T, Su TP, Betenbaugh MJ (2014) Bcl-2 family in inter-organelle modulation of calcium signaling; roles in bioenergetics and cell survival. *J Bioenerg Biomembr* 46(1):1–15.
34. Pinton P, Rizzuto R (2006) Bcl-2 and Ca^{2+} homeostasis in the endoplasmic reticulum. *Cell Death Differ* 13(8):1409–1418.
35. Rong YP, et al. (2009) The BH4 domain of Bcl-2 inhibits ER calcium release and apoptosis by binding the regulatory and coupling domain of the IP3 receptor. *Proc Natl Acad Sci USA* 106(34):14397–14402.
36. Monaco G, et al. (2012) Selective regulation of IP3-receptor-mediated Ca^{2+} signaling and apoptosis by the BH4 domain of Bcl-2 versus Bcl-Xl. *Cell Death Differ* 19(2): 295–309.
37. Rong YP, et al. (2008) Targeting Bcl-2-IP3 receptor interaction to reverse Bcl-2's inhibition of apoptotic calcium signals. *Mol Cell* 31(2):255–265.
38. Chang MJ, et al. (2014) Feedback regulation mediated by Bcl-2 and DARPP-32 regulates inositol 1,4,5-trisphosphate receptor phosphorylation and promotes cell survival. *Proc Natl Acad Sci USA* 111(3):1186–1191.
39. Sung PJ, et al. (2013) Phosphorylated K-Ras limits cell survival by blocking Bcl-xL sensitization of inositol trisphosphate receptors. *Proc Natl Acad Sci USA* 110(51): 20593–20598.
40. Ku B, Liang C, Jung JU, Oh BH (2011) Evidence that inhibition of BAX activation by BCL-2 involves its tight and preferential interaction with the BH3 domain of BAX. *Cell Res* 21(4):627–641.
41. Fletcher JI, et al. (2008) Apoptosis is triggered when prosurvival Bcl-2 proteins cannot restrain Bax. *Proc Natl Acad Sci USA* 105(47):18081–18087.
42. Kvansakul M, Hinds MG (2015) The Bcl-2 family: Structures, interactions and targets for drug discovery. *Apoptosis* 20(2):136–150.
43. Mak DO, Foskett JK (2015) Inositol 1,4,5-trisphosphate receptors in the endoplasmic reticulum: A single-channel point of view. *Cell Calcium* 58(1):67–78.
44. Fan G, et al. (2015) Gating machinery of $InsP_3R$ channels revealed by electron cryomicroscopy. *Nature* 527(7578):336–341.
45. Oltersdorf T, et al. (2005) An inhibitor of Bcl-2 family proteins induces regression of solid tumours. *Nature* 435(7042):677–681.
46. Tzung SP, et al. (2001) Antimycin A mimics a cell-death-inducing Bcl-2 homology domain 3. *Nat Cell Biol* 3(2):183–191.
47. Chen L, et al. (2005) Differential targeting of prosurvival Bcl-2 proteins by their BH3-only ligands allows complementary apoptotic function. *Mol Cell* 17(3):393–403.
48. Rajan S, Choi M, Baek K, Yoon HS (2015) Bh3 induced conformational changes in Bcl-Xl revealed by crystal structure and comparative analysis. *Proteins* 83(7):1262–1272.
49. Feng W, Huang S, Wu H, Zhang M (2007) Molecular basis of Bcl-xL's target recognition versatility revealed by the structure of Bcl-xL in complex with the BH3 domain of Beclin-1. *J Mol Biol* 372(1):223–235.
50. Velmurugan GV, White C (2012) Calcium homeostasis in vascular smooth muscle cells is altered in type 2 diabetes by Bcl-2 protein modulation of $InsP_3R$ calcium release channels. *Am J Physiol Heart Circ Physiol* 302(1):H124–H134.
51. Deverman BE, et al. (2002) Bcl-xL deamidation is a critical switch in the regulation of the response to DNA damage. *Cell* 111(1):51–62.